Optical tomography based on nonredundant array scanning holography

Ping Sun (孙 萍)[1,2], Jinghui Xie (谢敬辉)[1], and Yuanlin Zhou (周元林)[1]

[1] *Department of Optical Engineering, Beijing Institute of Technology, Beijing 100081*
[2] *Department of Physics, Beijing Normal University, Beijing 100875*

Received January 21, 2003

A novel technique termed nonredundant array scanning holography based on the principle of optical heterodyne scanning holography and the tomographic technique of coded aperture imaging is proposed. The system designed in terms of this technique codes an object optically and decodes its coded image digitally. It can realize optical tomograms of three-dimensional objects. It also has potentially practical value due to its compact structure. The computer simulations present the principle of the technique. Some experiments at the proof-principle level are performed to test the principle.

OCIS codes: 170.6960, 170.1630, 170.0110, 070.6110.

Optical heterodyne scanning holography (OSH) proposed by T. C. Poon *et al.*[1] is a novel technique in which three-dimensional (3-D) information of an object can be recorded by two-dimensional (2-D) scanning. The technique involves optically scanning the 3-D object by a time-dependent Fresnel zone plate (TDFZP) generated by the superposition of a plane wave and a spherical wave of different temporal frequencies. The reconstruction of the hologram can be achieved using an electron-beam addressed spatial light modulator or performed numerically[2,3]. The OSH system has both advantages of optics and electronics. However, its complexity makes it difficult to be used in practice. In this paper, we use a nonredundant array (NRA) fabricated by heliography to replace the FZP coded aperture in OSH. The 3-D imaging system with a NRA coded aperture has good quality of reconstructed image contrast, because its point spread function (PSF) has central spike and flat sidelobes. The background noises of the reconstructed images are reduced with the method of spatial filtering. The computer simulations demonstrate the principle of the system and some experimental results at the proof-principle level are achieved.

The setup of 3-D imaging system based on NRA scanning holography is shown in Fig. 1. The laser beams from semiconductor laser (λ_0=650 nm) become uniform after transmitting through a pinhole and the aperture A_1. The NRA aperture is located at depth z_1 away from the pinhole. The object with thickness D is located at depth z. Set a Cartesian coordinate system (x_1, y_1, z_1) with its origin at pinhole. Assume the intensity distribution of the NRA aperture is $I_1(x_1, y_1)$ at depth z_1. The light beam illuminates the NRA aperture and then a NRA projection is produced with intensity distribution $I_2(x, y; z)$ which is called the coded function. Assume a 3-D object with transmittance $O(x, y; z)$ can be divided into n discrete sections ($i = 1, 2, \cdots, n$). While the object is scanned, a photomultiplier tube (PMT) collects its transmitted light.

The hologram $H(x, y; z_i)$ coded by the NRA projection at depth $z = z_i$ section is the convolution of the ith sectional transmittance $O(x, y; z_i)$ of the object with the intensity distribution $I_2(x, y; z_i)$ of the NRA projection arriving at the depth $z = z_i$ section. $H(x, y; z_i)$ can be written as

$$H(x, y; z_i) = O(x, y; z_i) * I_2(x, y; z_i), \tag{1}$$

where $*$ is the convolution operator and $H(x, y; z_i)$ is termed as the scanning hologram of the section at depth z_i. The whole hologram of the 3-D object is the sum of all sectional hologram $H(x, y; z_i)$ given by

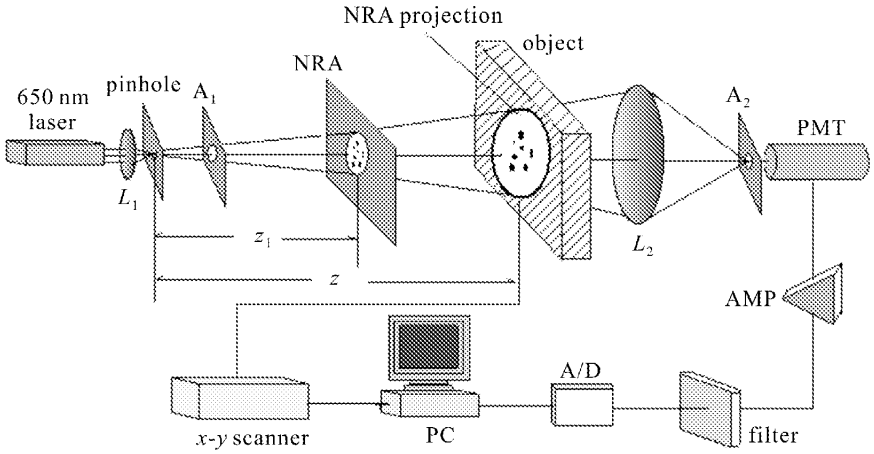

Fig. 1. Setup of 3-D imaging system based on NRA scanning holography.

$$H(x,y,z)=\sum_{i=1}^{n}H(x,y;z_i). \tag{2}$$

$H(x,y;z_i)$ becomes numerical signal after A/D transformation and then the hologram (or coded image) is performed digitally in a computer. The reconstructed image (or decoded image) can be obtained by correlating the scanning hologram with the decoding function. Assume the decoding function is $I_2'(x,y;z)$ and the decoding function of the section at depth $z=z_j$ is $I_2'(x,y;z_j)$. Decoding the $H(x,y;z)$ with $I_2'(x,y;z_j)$, we obtain the output image of the object as

$$\begin{aligned}\hat{O}(x,y;z)&=H(x,y;z)\star I_2'(x,y;z_j)\\&=O(x,y;z_j)*[I_2(x,y;z_j)\star I_2'(x,y;z_j)]\\&\quad+\sum_{i=1,i\neq j}^{n}\{O(x,y;z_i)\\&\quad*[I_2(x,y;z_i)\star I_2'(x,y;z_j)]\},\end{aligned} \tag{3}$$

where $\star$ is the correlation operator. The first term of Eq. (3) representing the case of $i=j$ gives us the reconstruction of the hologram of depth $z=z_j$ decoded with $I_2'(x,y;z_j)$. The second term representing the case of $i\neq j$ gives us the reconstruction of the hologram of depth $z\neq z_j$ with the decoding function of depth $z=z_j$. Generally, for the system using the NRA as coded and decoded aperture, the correlation $I_2(x,y;z_j)\star I_2'(x,y;z_j)$ becomes the autocorrelation of $I_2(x,y;z_j)$, if the depth z_j of decoding function is equal to that of the coding function, i.e. $z_j=z_i$. Also, the correlation $I_2(x,y;z_j)\star I_2'(x,y;z_j)$ is called the system PSF. In this case, the PSF is similar to a 2-D Dirac delta function $\delta(x,y;z_j)$. As a result, we obtain the reconstructed image of 3-D object at depth $z=z_i$ section from the first term of Eq. (3). However, the correlation of the second term of Eq. (3) represents the sum of cross correlations of $I_2'(x,y;z_j)$ with all sectional coding function $I_2(x,y;z_i)$ except that of z_i section, which degrades the δ function. Consequently, the second term refers to the background noises. Thus, Eq. (3) can be rewritten simply as

$$\hat{O}(x,y;z)=O(x,y;z_j)+N(x,y;z), \tag{4}$$

where $N(x,y;z)$ represents the quasi uniform background noises. Equation (4) indicates that if we use the decoding function of a particular section to decode the scanning hologram of the 3-D object, we derive the clear reconstructed image of this section and the blurry images of other sections. Hence, the different sectional tomograms can be extracted when the depth z of the decoding function is selected.

A NRA means that each separation between all possible pairs of holes in an array will occur only once, and thus the separations are nonredundant[4]. According to the definition we compile a program with the Visual C++ to design the NRA. Let the NRA be 64 × 64 pixels, thus we obtain forty-six nonredundant holes. Figures 2(a) and (b) show the pattern of the NRA and its normalized autocorrelation function respectively. As shown in Fig. 2(b), the autocorrelation consists of a central spike with the flat sidelobes. This flat

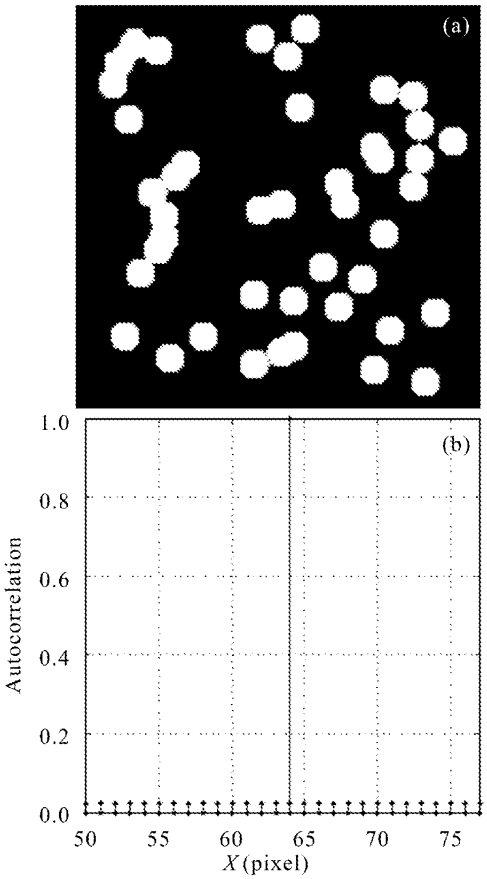

Fig. 2. Designing of the NRA. (a) Pattern of the NRA of 64 × 64 pixels; (b) 1-D slice through the normalized autocorrelation function of the NRA.

background will introduce a white noise into the decoded image, but it can be reduced with spatial filtering in frequency domain.

Let the ith$(i=1,2,\cdots,N)$ hole in the NRA be represented by $f_i(\cdot)$

$$f_i(\cdot)=\left\{\begin{array}{ll}0, & \text{if}(x-\xi_i)^2+(y-\eta_i)^2>r_i^2\\1, & \text{if}(x-\xi_i)^2+(y-\eta_i)^2\leq r_i^2\end{array}\right\}. \tag{5}$$

The transmittance function of a NRA aperture at depth z_1 with N holes becomes

$$I_1(x_1,y_1)=\sum_{i=1}^{N}f_i(\cdot), \tag{6}$$

where r_i is the radius, ξ_i and η_i represent the Cartesian coordinates of center of the ith hole, and here N is equal to 46.

From simple geometry, the coded function $I_2(x,y;z_i)$ is the magnified version of $I_1(x_1,y_1)$. Given by

$$I_2(x,y;z_i)=I_2(x_1,y_1,a)=\sum_{i=1}^{n}f_i'(\cdot), \tag{7}$$

where $f_i'(\cdot)$ is determined by the magnification factor $a=z/z_1$. The decoding function $I_2'(x,y;z_i)$ is equal to the coded function.

Computer simulations are performed to present the principle. An input image with array size of 100 × 100

pixels is designed shown in Fig. 3(a), in which the diameter of the circle is 10 pixels. The coded image shown in Fig. 3(b) is generated numerically using Eqs. (1) and (7). The decoded image surrounded by the background using Eqs. (3) and (7) (let $a = 1$) is shown in Fig. 3(c). According to the concept of spatial filtering, the approximate white background noises locate at the center in frequency domain and mix with the low frequency information of the object. A high pass filter (HPF) is valid to eliminate this kind of noise. Here, the diameter of a central stop of the HPF is designed to be 3 pixels. The filtering process consists of three steps. First, transform the decoded image shown in Fig. 3(c) by Fourier transformation (FT). Secondly, multiply the FT of the decoded image with the HPF. Last, transform the result above into spatial domain by inverse FT. The last result is the decoded image with spatial filtering illustrated in Fig. 3(d). Note that the most of background noises are suppressed and the signal-to-noise ratio of the circle becomes better. Change $a = 1$ to $a = 2$ in Eq. (7), in other words, let depth z of the decoding function be mismatched with that of coded function, we get a blurry decoded image like Fig. 3(e). This fact indicates that the decoded image of a particular section can be extracted only if the depth z of the decoding function is matched with that of the coding function.

After simulations, we design and set up a 3-D imaging system as shown in Fig. 1. Take a transparency as an object on which there is a circle with diameter of 8 mm. The NRA aperture with hole diameter of 1.5 mm is located at depth z_1=60 cm. Place the transparency at z=62 cm and z'=70 cm respectively. During experiments, the object moves in a 2-D way driven by an $x - y$ scanner. The scanning area is 5×5 cm^2 and the whole time takes 20 s. Figures 4(a) and (d) show the coded images of the transparency at depth $z = 62$ cm and $z' = 70$ cm, respectively. Figures 4(b) and (e) are the decoded images with different decoding functions. It can be seen the decoded images of the object with strong background noises. Figures 4(c) and (f) show the decoded images of Fig. 4(b) and (e) with spatial filtering respectively. From above figures, the circle is extracted from the background and the background noises are suppressed. The experiments verify the tomographic function of the 3-D imaging with NRA coded aperture.

In fact the decoded images in Figs. 4(b) and (e) are also affected by other factors such as mechanical vibration of the $x - y$ scanner and intensity floating of the laser. Consequently, the noise intensity of the decoded images in experiments is stronger than that in simulations. In addition, if the number of holes of the NRA increases, there will be a sharp decoded image and the background of the decoded image will become more homogeneous without increasing appreciably in intensity[5,6].

We have shown the principle of the 3-D imaging system based on NRA scanning holography. The coded image of a 3-D object is recorded optically and the decoded image is performed digitally, thus the system can deal with the reconstructed images by means of advanced technique of digital images like spatial filtering in frequency domain. The system is possible to be used in practice for its compact structure. Both simulations and experiments show that the system offers some possibilities for 3-D tomographic imaging.

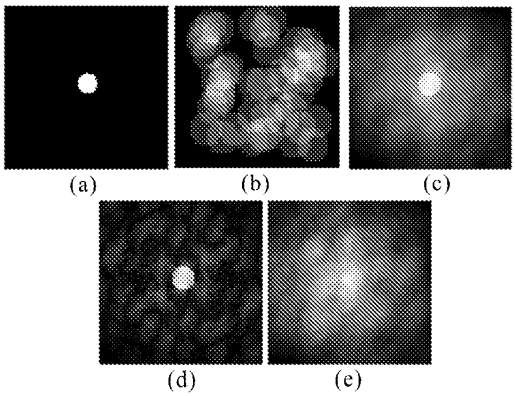

Fig. 3. Computer simulations. (a) Original image; (b) coded image; (c) decoded image; (d) decoded image with high-pass filtering; (e) decoded image with z mismatching.

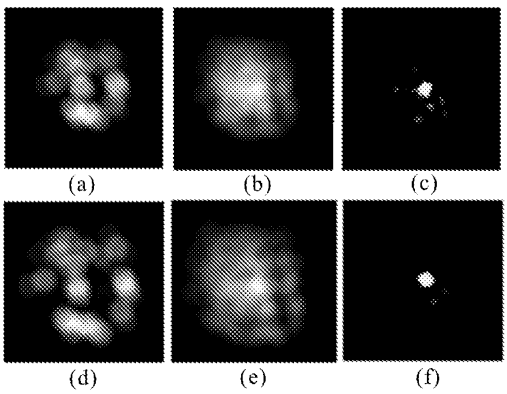

Fig. 4. Experimental tomograms. (a), (b) and (c) Coded image, decoded image and decoded image with spatial filtering at depth $z = 62$ cm; (d), (e) and (f) coded image, decoded image and decoded image with spatial filtering at depth $z' = 70$ cm.

We thank Guangdong Well Medical Science and Technology Corporation of China for its support. P. Sun's e-mail address is pingsun145@sina.com.

References

1. T. C. Poon, B. W. Schilling, K. B. Doh, M. H. Wu, K. Shinoda, and Y. Suzuki, Opt. Eng. **34,** 1338 (1995).
2. T. C. Poon, B. W. Schilling, M. H. Wu, K. Shinoda, and Y. Suzuki, Opt. Lett. **18,** 63 (1993).
3. B. W. Schilling and G. C. Templeton, Appl. Opt. **40,** 5474 (2001).
4. E. E. Fenimore and T. M. Cannon. Appl. Opt. **17,** 337 (1978).
5. A. Wouters, K. M. Simon, and J. G. Hirschberg, Appl. Opt. **12,** 1871 (1973).
6. K. S. Han, G. J. Berzins, D. S. Mason, and D. G. Langner, Appl. Opt. **16,** 1260 (1977).